NASA TECHNICAL MEMORANDUM

NASA TM-78861

NASA TM-78861

SENSITIVITY OF 30-CM MERCURY BOMBARDMENT ION THRUSTER CHARACTERISTICS TO ACCELERATOR GRID DESIGN

by V. K. Rawlin
Lewis Research Center
Cleveland, Ohio 44135

TECHNICAL PAPER to be presented at the
Thirteenth International Electric Propulsion Conference
cosponsored by the American Institute of Aeronautics and Astronautics
and the Deutsche Gesselschaft fur Luft-und Raumfahrt
San Diego, California, April 25-27, 1978

AIAA 78-668

SENSITIVITY OF 30-CM MERCURY BOMBARDMENT ION THRUSTER CHARACTERISTICS TO ACCELERATOR GRID DESIGN

by V. K. Rawlin

National Aeronautics and Space Administration
Lewis Research Center
Cleveland, Ohio 44135

TECHNICAL PAPER to be presented at the

Thirteenth International Electric Propulsion Conference
cosponsored by the American Institute of Aeronautics and Astronautics
and the Deutsche Gesselschaft fur Luft-und Raumfahrt
San Diego, California, April 25-27, 1978

SENSITIVITY OF 30-CM MERCURY BOMBARDMENT ION THRUSTER CHARACTERISTICS TO ACCELERATOR GRID DESIGN

by V. K. Rawlin

National Aeronautics and Space Administration
Lewis Research Center
Cleveland, Ohio 44135

E-9591

ABSTRACT

The design of ion optics for bombardment thrusters strongly influences overall performance and lifetime. The operation of a 30-cm thruster with accelerator grid open area fractions ranging from 43 to 24 percent, was evaluated and compared with previously published experimental and theoretical results. Ion optics properties measured included the beam current extraction capability, the minimum accelerator grid voltage to prevent backstreaming, ion beamlet diameter as a function of radial position on the grid and accelerator grid hole diameter, and the high energy, high angle ion beam edge location. Discharge chamber properties evaluated were propellant utilization efficiency, minimum discharge power per beam amp, and minimum discharge voltage.

INTRODUCTION

The design of the ion optics dramatically impacts overall ion thruster performance and lifetime (refs. 1 to 4). The ion optics design and operating voltages affect the discharge chamber performance by influencing the propellant utilization efficiency, power efficiency, and the minimum discharge voltage. The discharge voltage in turn, directly affects discharge chamber component lifetime. The grid design also specifies the current carrying capability of the grids themselves and is a fundamental determinant of the maximum thrust to power ratio and thrust density of a bombardment thruster. This paper extends the initial information presented in references 3 and 5 regarding the sensitivity of 30 cm thruster characteristics to ion optics having accelerator grid holes smaller in diameter than those of the screen grid.

APPARATUS

Thrusters and Optics

For the efforts described herein, ion optics with five different geometries were evaluated and compared with previously published

performance of other grid geometries. Descriptions of all of the ion optics geometries tested and used for comparison are listed in table I.

As table I shows, the major parameters evaluated were the accelerator grid (downstream grid) hole diameter and the accelerator grid open area fraction. Variation of this dimension was selected since it has been shown to strongly affect many thruster characteristics. Two 30-cm thruster designs were used. They were both equivalent to the Engineering Model Thruster (EMT, ref. 4) design with the exception that one thruster had electromagnets in place of the standard permanent magnets. All of the tests were conducted in the 3.0-m-diameter bell jar of the 7.6 m diameter by 21.4 m long vacuum tank at Lewis Research Center.

Power Supplies

Two types of power supplies were used for the tests presented.

Laboratory supplies. - The laboratory power supplies were 60 hertz input supplies. The screen and accelerator high-voltage supplies were a high capacity, three phase, full wave bridge rectifier design. The discharge, magnetic baffle, and two keeper supplies were full wave, single phase rectified d.c. sources. The six resistive heaters were powered with alternating current.

Series resonant inverter. - Other tests were conducted using an SCR series resonant inverter power processor similar to that described in reference 6. This ppu has 12 flight type power supplies. While the specific design, such as output impedance, of the resistive load supplies does not significantly affect thruster control or operation, this is not necessarily true of the plasma load supplies. Pertinent characteristics of the five plasma load supplies are given in reference 7.

Beam Ion Probes

Probes were used to measure the ion flux due to low energy charge exchange ions and high angle, high energy ions. Details of the construction and location of the probes are given in figure 1. The probes were located 7.2 cm radially outward from and 0.63, 2.54, and 4.44 cm downstream of the outermost accelerator grid holes. The centers of the probes were at angles of 85°, 71°, and 58° with respect to the last accelerator grid hole.

Each molybdenum planar probe had a diameter of 1.28 cm and was covered by a retarding potential grid (70 percent open) with a 0.95 cm diameter entrance hole. The probes were all mounted in an

outer case which had an electron retarding grid, also 70 percent open. Thus the effective collection area of each probe was about 0.35 cm^2.

Electrically, the probes were tied to facility ground through sensing resistors. The outer case was always biased 10 volts negative with respect to ground to repel neutralizer electrons. The retarding potential was variable from 0 to ±1 kV.

PROCEDURE

The following properties were measured for the various accelerator grid designs presented in table I.

(a) Ion plasma

(1) Minimum total accelerating voltage (voltage difference between positive plasma and negative accelerator grid) required to extract a given beam current.

(2) Minimum accelerator grid voltage necessary to prevent electrons from backstreaming into the discharge chamber.

(3) Maximum net-to-total accelerating voltage ratio (net accelerating voltage is voltage difference between discharge plasma and ground).

(4) Individual beamlet (ion beam from single hole) diameter as a function of accelerator grid hole diameter.

(5) Low energy charge exchange ion flux.

(6) Beam edge location for low density, high energy, high angle ions.

(b) Discharge chamber performance

(1) Propellant utilization efficiency.

(2) Minimum discharge power losses per beam ampere.

(3) Minimum value of discharge voltage for fixed beam and discharge currents.

RESULTS AND DISCUSSION

Lifetime and performance are two of the most important properties of ion thrusters. References 8 and 9 have shown that the present life-limiting phenomenon of 30 cm thrusters is erosion of the screen grid by discharge chamber ions. Reductions of the discharge voltage, through the use of Small Hole Accelerator Grids (SHAG), has been shown to reduce screen grid erosion (refs. 2 and 10). Thruster performance is most strongly affected by the efficiency of ion production

(propellant and power efficiencies) and the ability to extract the ions once they are produced. To obtain the maximum thrust for a given input power, it is desirable to minimize the discharge chamber losses and extract the maximum possible beam current with the least amount of net accelerating voltage. However, second order effects, such as thrust losses due to beam divergence and multiply charged ions may increase for these operating conditions. Lifetime and physical limitations should also be considered. The sensitivity of these parameters to ion optics designs was investigated and the results are presented below.

Perveance

The current carrying capability of a set of ion optics is measured by a parameter called "perveance" or for a single aperture "normalized perveance" (ref. 1). For a given grid geometry and propellant type, perveance values can be obtained by determining the minimum total voltage required to extract the desired beam current without appreciable ion impingement on the accelerator grid due to ion defocusing. Figure 2 compares the theoretical total voltage requirements to avoid accelerator impingement as a function of accelerator grid hole diameter (ref. 11) with those obtained experimentally. As figure 2 shows, the voltage required increases as the accelerator grid hole diameter decreases. This is referred to as a "loss of perveance." The experimental and theoretical results are in rough agreement. The differences are probably due to the assumptions and techniques used for the theoretical results (i.e., trajectories of singly charged ions from a single aperture with a grid spacing of 0.64 mm were used). Experimentally, there is a high fraction of multiply charged ions at the thruster centerline which require less voltage to obtain the same current. Also, the experimental results had a cold grid spacing of 0.62 ± 0.05 mm but, when heated during operation, this spacing was probably reduced thereby yielding a higher perveance.

The loss of perveance experienced with accelerator hole reduction may be recovered by reducing the accelerator grid thickness or using a smaller grid spacing, as suggested in reference 12.

Ratio of Net-to-Total Voltage

References 1 and 11 have indicated that the ratio of net-to-total accelerating voltage, R, is also sensitive to the accelerator grid hole diameter. The maximum value of R, R_{MAX}, occurs when the accelerator grid voltage is at its minimum value. R_{MAX} is specified by the onset of electrons backstreaming from the beam into the discharge chamber. The minimum value of R, R_{MIN}, occurs when the net accelerating voltage is so low that a large quantity of ions are

defocused and impinge on the accelerator grid causing excessive erosion.

Maximum R. - Operation at high values of R reduces the flux of accelerator grid material sputtered by impinging charge exchange ions and the thrust losses due to ion beam divergence.

Kaufman (ref. 1) has correlated the theoretical data of Lathem (ref. 13) for R_{MAX} with the ratio of accelerator grid thickness to hole diameter. This is shown in figure 3 and compared with experimental results. The generalization parameter, (the minimum accelerator grid voltage multiplied by the grid spacing divided by the total voltage and the accelerator grid hole diameter, $(V_{AMIN}/V_T)(l_g/d_A)$), has a value of $1/2\pi$, from Spangenberg (ref. 14), for the ideal geometry of zero accelerator grid thickness. Theoretically, there was little change of R_{MAX} with ion current (or perveance), but, experimentally, there was about a 15 percent increase in the required minimum accelerator grid voltage as the perveance doubled. The difference between the theoretical and experimental results is most probably due to the finite thicknesses of actual ion optics and to different assumed values of grid separation distance and field strength in any given aperture region. Actual ion optics are multiaperture systems where the grid separation is small with respect to grid hole diameters. Thus, the field strength based on actual grid separation is obviously greater than would be found in the aperture region. If a larger value of l_g had been used to calculate the generalization parameter for the experimental results, the agreement would be better.

Figure 4 shows R_{MAX} plotted simply as a function of the accelerator grid hole diameter. In general, R_{MAX} increases as the hole diameter decreases. For small values of hole diameter, the voltage required to prevent electron backstreaming increases because the total voltage required also increases, as in figure 2, and R_{MAX} tends to remain constant at a value near 0.9. Figures 3 and 4 can be used to determine the minimum accelerator grid voltage allowed after the grid hole diameter and beam current are specified.

Minimum R. - There may be missions for electric propulsion where it is very desirable to obtain the maximum thrust per module. For a given beam power, the maximum thrust occurs at the maximum beam current and lowest net accelerating voltage. As the beam current increases, the total voltage must also increase according to the perveance relationship. Low values of net accelerating voltage imply operation at low values of $R \cdot R$ is limited at the point R_{MIN}, where excessive ion overfocusing causes large accelerator impingement current and intolerable grid erosion. Figure 4 also shows R_{MIN} as a function of the accelerator grid hole diameter. Since the determination of R_{MIN} depends on focusing, R_{MIN} is sensitive to the amount of intentional grid hole pattern misalinement ("compensa-

tion," ref. 15) which accounts for the data spread at a hole diameter of 1.91 mm. With proper compensation R_{MIN} appeared to be insensitive to accelerator grid hole diameter. This, again, is probably due to the fact that as the accelerator grid hole is decreased and more total voltage is required, the minimum beamlet diameter also decreases and R_{MIN} remains nearly constant. For a given grid, R_{MIN} was insensitive to changes in beam current from 1.0 to 3.0 amps.

References 1, 11, and 15 have shown that operation at low values of R increase the ion beam divergence losses due to defocusing. However, recent efforts, using a decelerator grid, have demonstrated a reduction in beam spread and R_{MIN} (refs. 16 and 17).

Figures 2 and 4 can be used to determine maximum allowable accelerator grid voltage, for two grid optics, after the accelerator hole diameter and beam power have been specified.

Minimum Ion Beamlet Diameter

It has been shown in reference 1 that the theoretical ratios of minimum ion beamlet diameter to screen hole diameter are primarily functions of the normalized perveance and hole shape. It was also noted that the location of this minimum is a function of the perveance and R at low values of perveance. In general, the ratios of the minimum beamlet diameter and the location of the minimum to the screen hole diameter decreased with normalized perveance.

Experimentally, the primary concern is the beamlet diameter within the accelerator hole or beamlet exit diameter. For three sets of ion optics, having the same screen grid hole diameter and grid spacing but different accelerator hole diameters, thin tantalum foil was placed on the downstream side of the accelerator grid. The grids were operated at the same constant conditions of a 2.0 ampere beam, net accelerating voltage of 1140 volts and an R of 0.79. Figure 5 shows the variation of the resulting hole diameter as a function of radial position (or perveance). The beamlet exit diameter was nearly constant for a given accelerator hole size even though the current per hole or perveance varies considerably with radius. Figure 5 also shows that as the accelerator grid hole diameter was reduced, the ratio of maximum beamlet exit diameter to accelerator hole diameter was nearly constant at a value of 0.6. This suggests that further reductions of the accelerator grid hole diameter are possible. Trajectory analyses, presented in reference 18, indicated that the beamlet exit to grid hole diameter ratio increased to 1.0 as the grid hole decreased to 0.81 mm. But when optics with an accelerator grid hole diameter of 0.69 mm were built and tested in reference 5, they could be operated satisfactorily, provided the total voltage was more than that specified by the perveance limit.

Beam Edge Studies

As mentioned earlier, the accelerator grid hole diameter and discharge voltage have been reduced for the EMT in order to increase thruster lifetime without sacrificing performance. Tests were conducted to determine what effects, if any, these changes had on the magnitude and direction of ions near the thruster. Reference 19 showed that ion fluxes at high angles could be due to poorly focused thrust ions and charge exchange ions. The location of the charge exchange reaction determined the final ion energy.

Charge exchange ions. - Low density charge exchange ions, emanating from thrusters at high angles, may interact with nearby spacecraft surfaces. Low energy mercury ions striking conducting surfaces would be neutralized and may condense there. High energy ions would cause sputter erosion.

Reference 20 has measured and modeled both the ion currents resulting from charge transfer reactions between thrust ions and mercury atoms and the high energy, high angle ion flux from a 30-cm EMT. The motion of low energy charge exchange ions is predominantly radial. High energy (>100 eV), high angle ion flux was also found to exist at angles near 90°, with densities of about 10^{-8} amp/cm^2, and was found to be sensitive to R (net-to-total accelerating voltage ratio). In that study, it was suggested that these high energy, high angle ions were mostly the result of charge transfer reactions, which occurred in the grid interspace. Thus, being formed at relatively low R, their energy would be less than the net ion energy of the thrust ion beam. On the other hand, reference 18 has experimentally measured these "fringe" ions, at angles up to 80°, as having the full beam energy. They concluded that these ions were not poorly focused high energy charge exchange ions but were related to the end effect at the beam edge where the virtual ground neutralization plane curves away from the accelerator grid. Trajectory analyses for beam edge ions were in agreement with experimental results. Ions of both types probably exist at high angles.

Tests were conducted, in the program presented herein, to compare the high angle ion flux, from the EMT grid design, with that from an EMT using grid set 2. Three probes, capable of performing retarding potential analyses, were used as described in the Apparatus and Procedure section.

Low energy charge exchange ion flux. - Figure 6 shows the ion current densities measured as a function of the retarding potential. These data are typical of EMT and SHAG designs. Three noteworthy features of figure 6 are: the current densities are of the order $1\text{-}2\times10^{-6}$ A/cm^2, the current density increases with axial distance, and ion energies are primarily between 2-3 eV. These results were as expected from reference 20.

High energy ion flux. - With a retarding potential of +6 volts, the current measured by the probes was primarily due to high energy ions. In fact, when the retarding potential was increased from 6 to 1000 volts the probe currents remained nearly the same. Figure 7 shows the high energy ion current densities as a function of accelerator grid voltage for ion optics with accelerator grid hole diameters of 1.52 mm and 1.27 mm. At the normal operating accelerator grid voltage of 340 volts, the current density is higher for the grid with the larger holes. But the SHAG optics appear to be more sensitive to variations in accelerator grid voltage, or R. Tests with other EMT optics indicated that fabrication, spacing, or alinement tolerances may be important in this respect. However, for all grids tested, the low density beam edge (10^{-6} ma/cm^2 or less) for the nominal net and total accelerating voltages of 1100 and 1440 volts, respectively, was measured to be at an angle of 55±4°. Thruster hardware within this angle, such as the ground screen and neutralizer, will be impinged upon by high energy ions.

One last feature of the high energy high angle ions, found in this study, was that the probe current versus accelerator grid voltage relationship was not sensitive to beam current. The minimum value of probe current increased, as the beam current was raised from 1.0 to 2.0 amps, but the voltage at which the probe current began to rise did not change. This is in agreement with results presented earlier for R_{MIN}.

Propellant Utilization Efficiency

References 3 and 5 have shown, that for fixed discharge losses, the measured discharge chamber propellant utilization efficiency will increase if the accelerator grid open area is reduced. This is due to the reflection of neutral mercury atoms back into the discharge chamber where they may be ionized. Reference 3 has also shown that discharge chamber performance improves when the screen grid open area is increased, providing a high transmission coefficient for ions. Those conclusions were found to be true for the ion optics used in this program, the results of which are presented in figure 8.

Comparing the performance of various grid sets, it is seen that EMT grids operated with a discharge voltage of 36 volts are similar in performance to grid sets 1 and 2 operated at 32 and 33 volts, respectively. The trade of reducing discharge voltage to hold constant performance can be used to reduce internal erosion. Reference 5 measured a 50 percent reduction in the ratio of doubly charged to singly charged ions by using SHAG optics and reducing the discharge voltage from 37 to 30 volts. The expected reduction of the erosion of discharge chamber components has since been measured (ref. 10).

Performance comparisons of grid sets 3 and 4 (identical in geometry except for grid dish direction) show the propellant utilization efficiency to be the same even though the discharge voltage was 32 volts for the grids dished out and 37 volts for the grids dished in.

Previous attempts to reduce the discharge losses (ref. 3) by increasing both grid open areas (grid sets 5 and 7) were successful but the maximum propellant utilization efficiency decreased. Figure 8 shows that grids with high screen grid open area and low accelerator grid open area (set 5) greatly improve discharge chamber performance.

Minimum Discharge Losses

Table II compares the minimum discharge chamber losses for grids which have the same screen grid design (67 percent open) but various accelerator open area fractions. As the accelerator open area was reduced the minimum discharge losses were also reduced, even when the discharge voltage was reduced and less multiply charged ions were present.

Minimum Discharge Voltage

Because erosion of discharge chamber components is a strong function of the discharge voltage (refs. 2, 8, and 10) the minimum discharge voltage, at which the thruster could be stably operated, was measured for several grid sets. The results are shown in figure 9. As the accelerator open area was reduced, the minimum discharge voltage was also reduced.

Lifetime

The addition of SHAG optics to the 900 series EMT, coupled with a reduction of discharge voltage to 32 volts, has been shown to reduce the screen grid erosion rate by about a factor of 3 (refs. 9 and 10) and thereby increase the expected thruster lifetime. Applying the results of reference 2 to the measured erosion rate, a lifetime of 15 000 hours is predicted (where lifetime is arbitrarily defined as the time required to erode 50 percent of the screen grid at full power). Increases in beam current (thrust level) will probably provide opportunities to trade increased performance for reduced lifetime.

Total Thruster Efficiency

The total thruster efficiency, corrected for multiply charged ions and beam divergence, is plotted as a function of specific impulse in figure 10, for both constant and variable input power. The performance of an EMT with SHAG optics is compared with that of the 900 series EMT. For data with SHAG optics the discharge voltage was 32 volts as compared with 36 volts for the EMT data. For both grid designs the discharge losses were 198 watts per beam amp and a neutralizer propellant flowrate of 30 equivalent mA was assumed.

Table III presents the values of beam current and voltage, R, and thrust factors used to calculate the efficiency, thrust, and specific impulse at constant input power. Corrections for multiply charged ions as a function of beam current were obtained using reference 18, while those for beam divergence, as a function of R, were obtained using reference 15. The lowest value of specific impulse was assumed to be limited by a value of R_{MIN} of 0.39 over the range of specific impulse shown, a thruster using SHAG optics is expected to be about 3.5 percent more efficient than the 900 series EMT.

Table IV gives the thruster parameters used to calculate the specific impulse, thrust, and efficiency for variable input power for an EMT operated with both grid designs. Data for the EMT were obtained from reference 7 while data from reference 5 were used to estimate the thrust correction factors used for SHAG optics. The use of SHAG improved the thruster efficiency over the 4:1 variation of input power. At full power and quarter power conditions the improvement is expected to be about 3.5 and 10 percent, respectively.

From figure 10 it is seen that, for either grid type, total thruster efficiency is nearly specified by the specific impulse regardless of input power. This occurs because increases in the product of the thrust factors, realized by reducing beam current and input power, are offset by lower values of propellant utilization efficiency. Likewise, decreases in the product of the thrust factors, obtained when the beam current is increased and R is decreased at constant input power, are nearly offset by increased propellant utilization efficiency.

CONCLUSIONS

The operation of a 30-cm mercury bombardment ion thruster, with ion optics having accelerator grid open area fractions ranging from 43 to 24 percent, was evaluated and compared with previously published experimental and theoretical results. The sensitivities of certain optics parameters, such as perveance, net-to-total accelerating voltage ratio, ion beamlet diameter, and high angle ion densities, to

accelerator grid hole diameter were documented. As the accelerator grid hole diameter was decreased it was found that:

1. The total accelerating voltage required to extract a given beam current increased.

2. The maximum net-to-total voltage ratio increased to 0.9 while the minimum ratio was nearly constant at 0.4.

3. The diameter of an ion beamlet exiting a typical accelerator grid hole was about 60 percent of the hole diameter.

4. The discharge losses and the minimum discharge voltage decreased.

5. The propellant utilization efficiency increased permitting trades to be made between performance and lifetime.

When the edge of the ion beam was investigated using grids with accelerator hole diameters of 1.52 mm (EMT) and 1.27 mm, it was found that:

1. The charge exchange ion current density ranged between 2.2 to 0.1 $\mu A/cm^2$ near the thruster for angles between 58° and 85° with respect to the beam axis.

2. The charge exchange ions were created at neutralizer keeper potential.

3. The directions of the high energy, high angle ions are a strong function of the net-to-total voltage ratio and at nominal operating voltages the density is about 0.3 mA/cm^2 at angles from the beam axis greater than 55°.

When EMT optics were replaced with grids having 1.14 mm diameter accelerator holes, the total thruster efficiency increased about 3.5 percent at the nominal full power conditions and 10 percent at quarter power. The lifetime in space, at full power conditions, is expected to be considerably in excess of 15 000 hours.

REFERENCES

1. Kaufman, H. R., "Technology of Electron-Bombardment Ion Thrusters," in "Advances in Electronics and Electron Physics," Vol. 36, Academic Press, Inc., New York, 1974, pp. 265-373.

2. Rawlin, V. K. and Mantenieks, M. A., "Effect of Facility Pressure on Internal Erosion of the 30-cm Mercury Ion Thruster," AIAA Paper 78-665, Apr. 1978.

3. Rawlin, V. K., "Performance of 30-cm Ion Thrusters with Dished Accelerator Grids," AIAA Paper 73-1053, Oct. 1973.

4. Masek, T. D., Poeschel, R. L., and Collett, C. R., "Evolution and Status of the 30-cm Engineering Model Ion Thruster," AIAA Paper 76-1006, Nov. 1976.

5. Vanrenkamp, R. P., "Characteristics of a 30-cm Thruster Operated with a Small Hole Accelerator Grid Ion Optics," AIAA Paper 76-1030, Nov. 1976.

6. Beiss, J. J. and Inouye, L. Y., "Power Processor for a 30 cm Ion Thruster," TRW Systems Group, Redondo Beach, Calif., TRW-20384-6002-RU-01, Oct. 1974 (NASA CR-134785).

7. Bechtel, R. T. and Rawlin, V. K., "Performance Documentation of the Engineering Model 30-cm Diameter Thruster," AIAA Paper 76-1033, Nov. 1976.

8. Mantenieks, M. A. and Rawlin, V. K., "Sputtering Phenomena of Discharge Chamber Components in a 30-cm Diameter Hg Ion Thruster," AIAA Paper 76-988, Nov. 1976.

9. Collett, C. R. and Bechtel, R. T., "An Endurance Test of a 900 Series 30-cm Engineering Model Ion Thruster," AIAA Paper 76-1020, Nov. 1976.

10. Collett, C. R., Private communication.

11. Poeschel, R. L., "High Power and 2.5 kW Advanced Technology Ion Thruster," Hughes Research Labs, Malibu, Calif., NASA CR-135163, Feb. 1977.

12. Rawlin, V. K., "Studies of Dished Accelerator Grids for 30-cm Ion Thrusters," AIAA Paper 73-1086, Oct. 1973.

13. Lathem, W. C., "Ion Accelerator Designs for Kaufman Thrusters," AIAA Paper 69-261, Mar. 1969.

14. Spangenberg, K. R., Vacuum Tubes, McGraw Hill, New York, 1948, p. 348.

15. Danilowicz, R. L., Rawlin, V. K., Banks, B. A., and Wintucky, E. G., "Measurement of Beam Divergence of 30-Centimeter Dished Grids," AIAA Paper 78-1051, Oct. 1973.

16. Meadows, G. A. and Free, B. A., "Effect of a Decel Electrode on Primary and Charge-Exchange Ion Trajectories," AIAA Paper 75-427, Mar. 1975.

17. Aston, G. and Kaufman, H. R., "Ion Beam Divergence Characteristics of Three-Grid Accelerator Systems," AIAA Paper 78-669, Apr. 1978.

18. Poeschel, R. L., "A 2.5 kW Advanced Technology Ion Thruster," Hughes Research Labs., Malibu, Calif., Apr. 1976 (NASA CR-135076).

19. Staggs, J. F., Gula, W. P., and Kerslake, W. R., "The Distribution of Neutral Atoms and Charge-Exchange Ions Downstream of an Ion Thruster," AIAA Paper 67-82, Jan. 1967.

20. Komatsu, G. K. and Stellen, J. M., Jr., "Beam Efflux Measurements," TRW Systems Group, Redondo Beach, Calif., June 1976 (NASA CR-135038).

TABLE I. - GRID GEOMETRIES

Grid	Hole diameter, mm		Open area fraction		Grid thickness, mm		Hole shape	Dish direction
	Screen (upstream grid)	Accelerator (downstream grid)	Screen	Accelerator	Screen	Accelerator		
EMT	1.91	1.52	0.67	0.43	0.38	0.51	Circular	Out
1	↓	1.14	↓	.24	↓	↓	↓	↓
2	↓	1.27	↓	.30	↓	↓	↓	↓
3	↓	1.27/[a]1.02	↓	.28	↓	↓	↓	↓
4	↓	1.27/[a]1.02	↓	.28	↓	↓	↓	In
5	2.08	1.22	.75	.27	↓	.38	Hexagonal	Out
[b]6	2.08	2.08	.75	.75	↓	↓	Hexagonal	↓
[b]7	1.91	1.91	.67	.67	↓	↓	Circular	↓

[a]1.27 mm holes for 0 to 7.5 cm radius, 1.02 cm holes out to edge.
[b]Data from refs. 3 and 12.

TABLE II. - MINIMUM DISCHARGE CHAMBER LOSSES

Acceleration grid open area fraction	Minimum discharge chamber losses, W/beam amp	Discharge voltage, V
0.67	180	37
.43	171	36
.30	170	33
.24	158	32

TABLE III. - THRUSTER PERFORMANCE, CONSTANT INPUT POWER, 2650 w

Grid design	Net voltage, V	Beam current, A	Net-to-total accelerating voltage ratio	Multiply charged ion thrust factor, α	Beam divergence thrust factor, F_t	Specific impulse, sec	Thrust, NT	Total thruster efficiency
900 EMT	1090	2.00	0.77	0.957	0.994	2892	0.1281	0.685
	920	2.30	.55	.955	.986	2644	.1332	.651
	722	2.79	.39	.950	.976	2319	.1417	.608
SHAG	1090	2.0	0.77	0.971	0.994	2998	0.1300	0.721
	920	2.30	.55	.968	.986	2738	.1358	.687
	722	2.79	.39	.966	.976	2409	.1441	.642

TABLE IV. - THRUSTER PERFORMANCE, 4:1 INPUT POWER RANGE

Grid design	Input power, W	Beam voltage, V	Beam current, A	Multiply charged ion thrust factor, α	Beam divergence thrust factor, F_t	Specific impulse, sec	Thrust, NT	Total thruster efficiency
900 EMT	2650	1100	2.00	0.957	0.994	2892	0.1281	0.685
	2250	1005	1.83	.959	.993	2672	.1119	.651
	1300	760	1.30	.974	.991	2159	.0702	.571
	660	605	.76	.986	.990	1625	.0368	.444
SHAG	2650	1100	2.0	0.971	0.994	2998	0.1309	0.721
	2250	1005	1.83	.974	.993	2844	.1137	.704
	1300	760	1.30	.983	.991	2403	.0708	.641
	660	605	.76	.997	.990	1967	.0372	.543

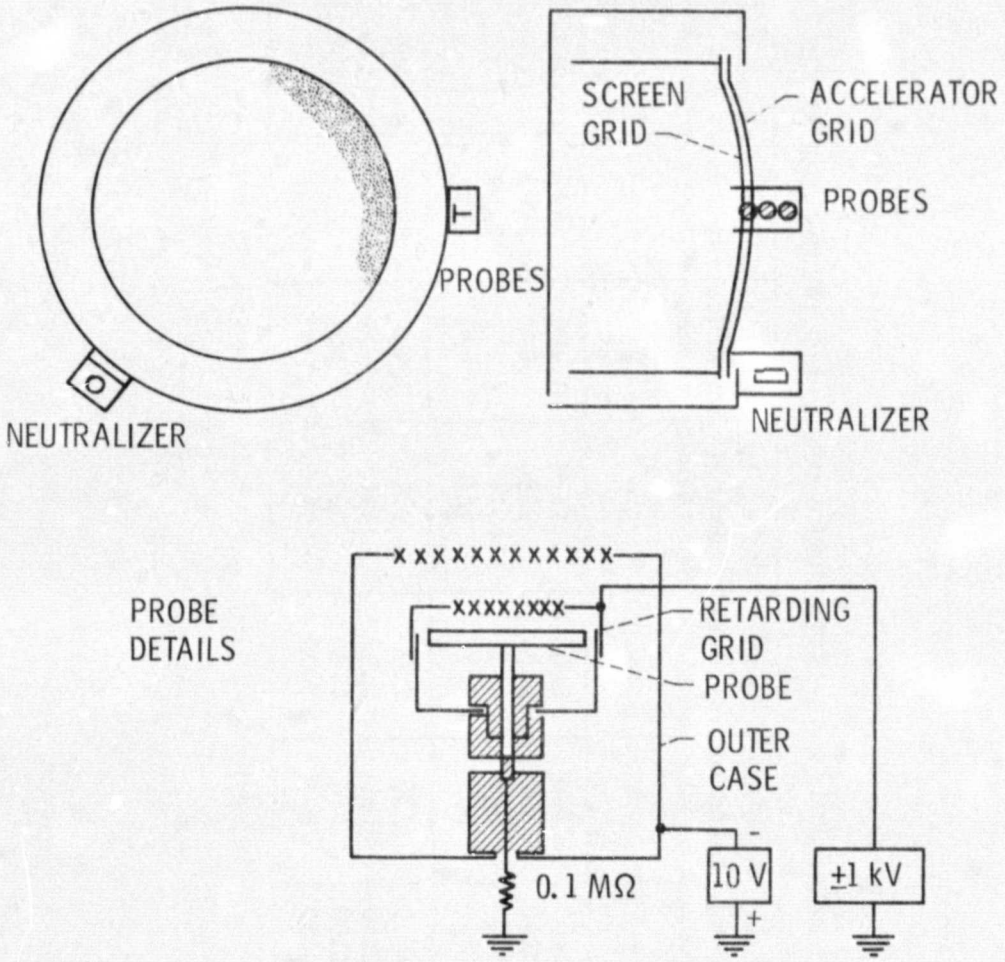

Figure 1. - Beam ion probes.

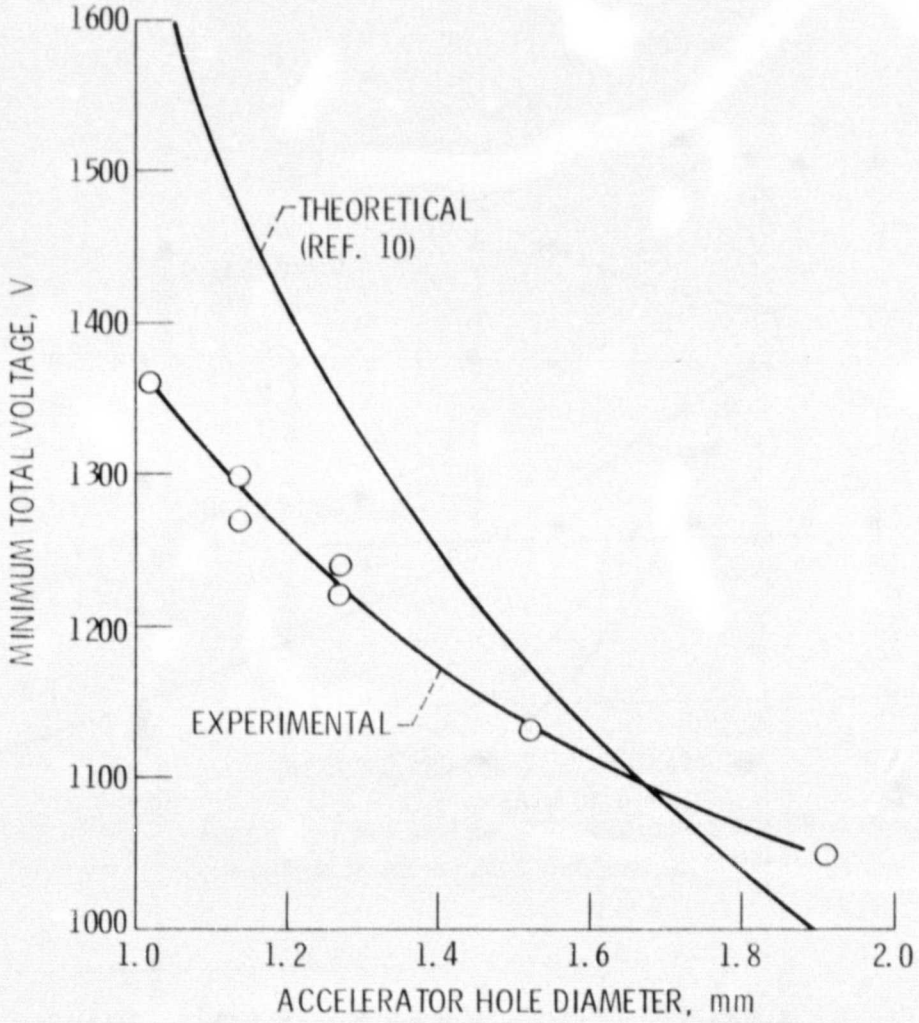

Figure 2. - Minimum total voltage as a function of accelerator hole diameter (beam current, 2 A).

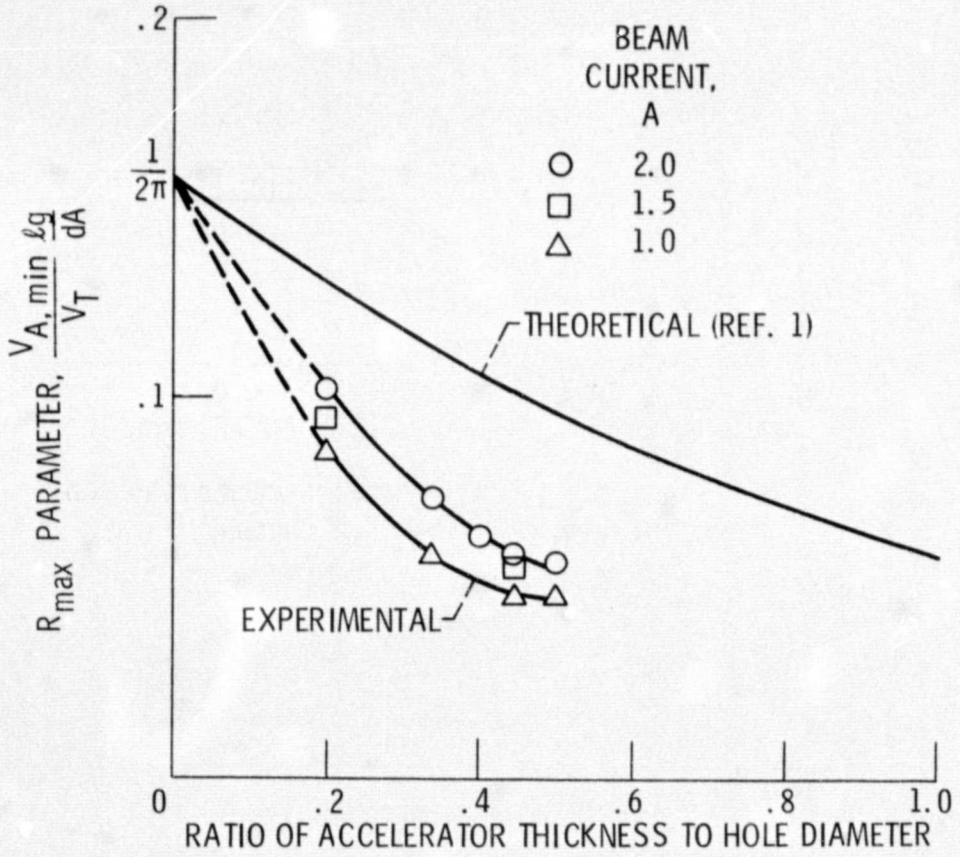

Figure 3. - R_{max} parameter as a function of accelerator thickness to hole diameter ratio.

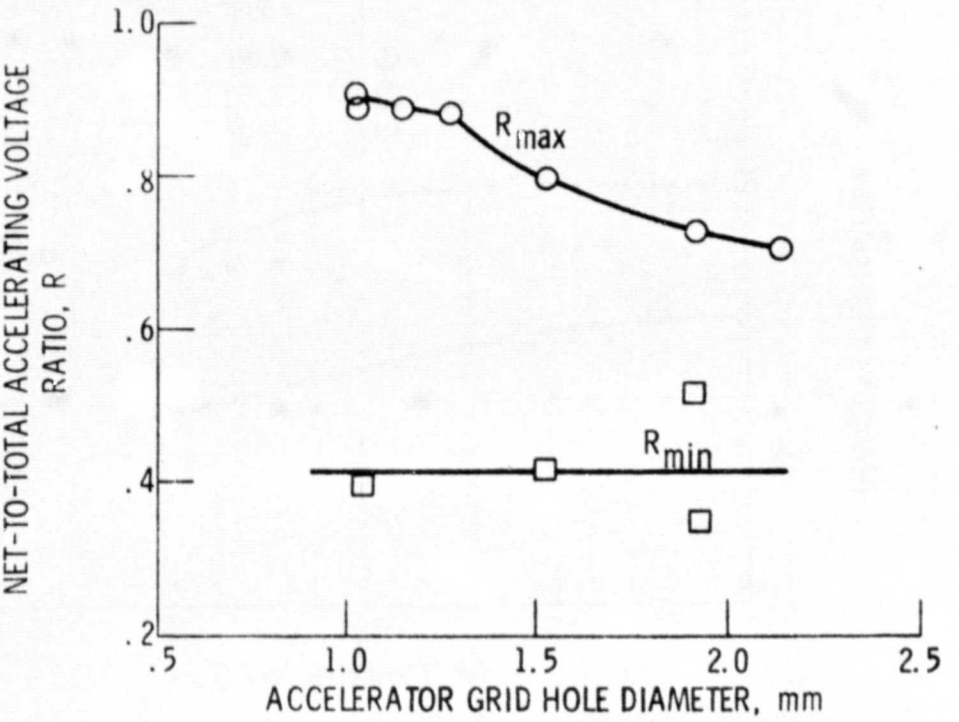

Figure 4. - Net-to-total accelerating voltage ratio as a function of accelerator grid hole diameter.

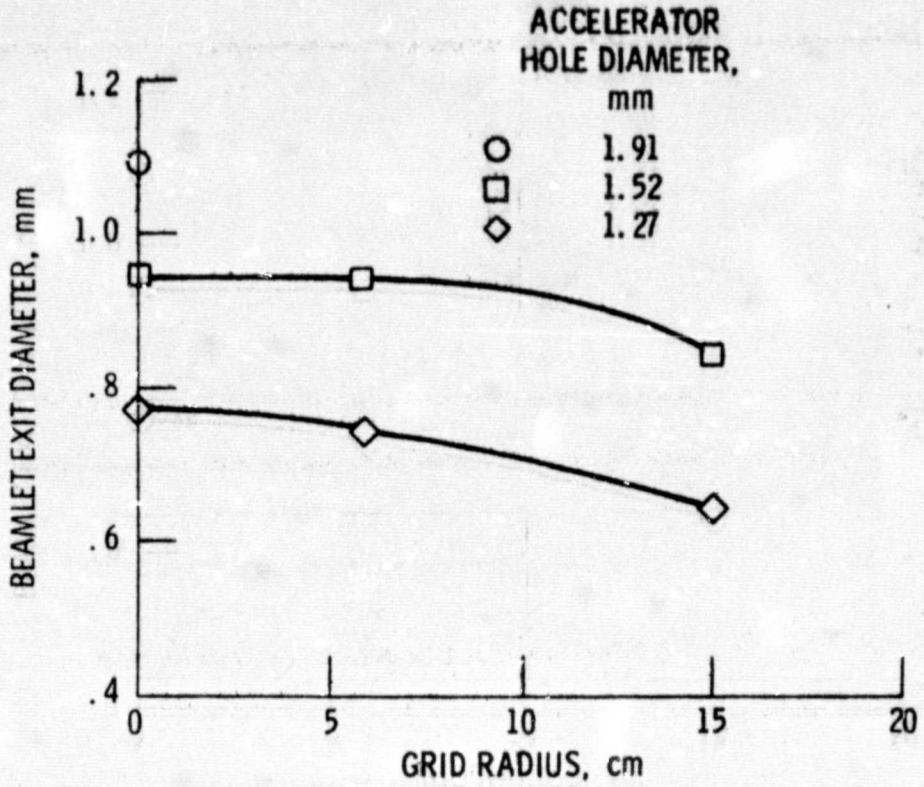

Figure 5. - Beamlet exit diameter as a function of grid radius (beam current, 2A; net voltage, 1140 V; R, 0.79).

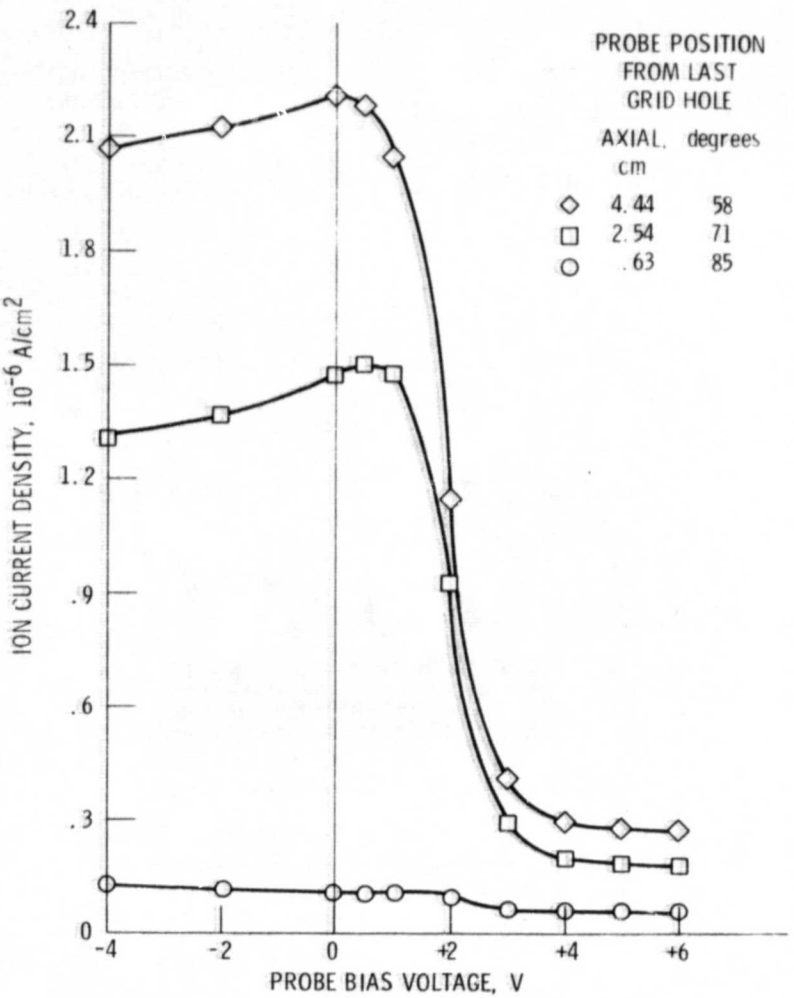

Figure 6. - Ion current density as a function of probe bias voltage (EMT with 1.27 mm SHAG optics, beam current, 2A; net voltage, 1100 V; R, 0.76; neutralizer keeper, 2 - 3 V above ground).

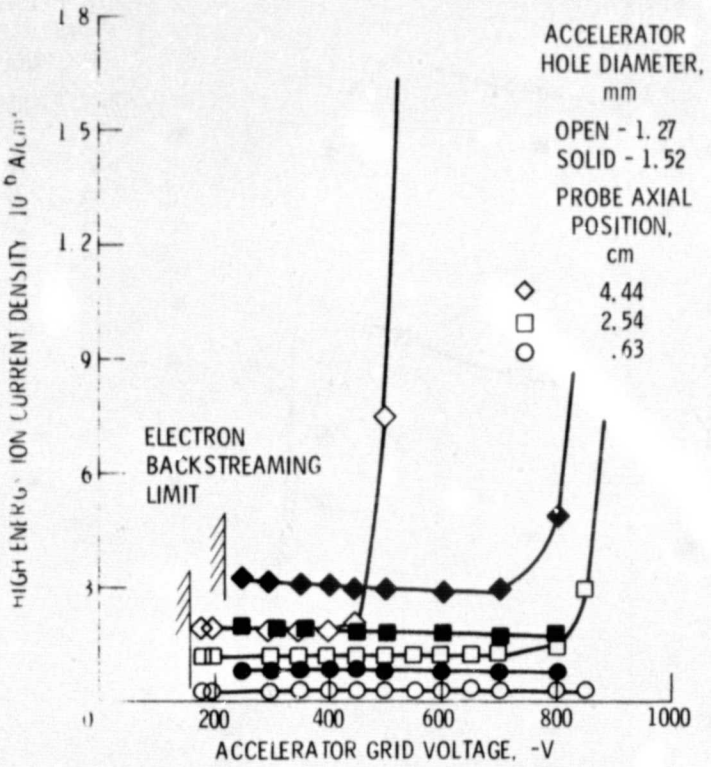

Figure 7. - Ion current density as a function of accelerator grid voltage (beam current, 2A; net voltage, 1100 V; probe bias, +6 V).

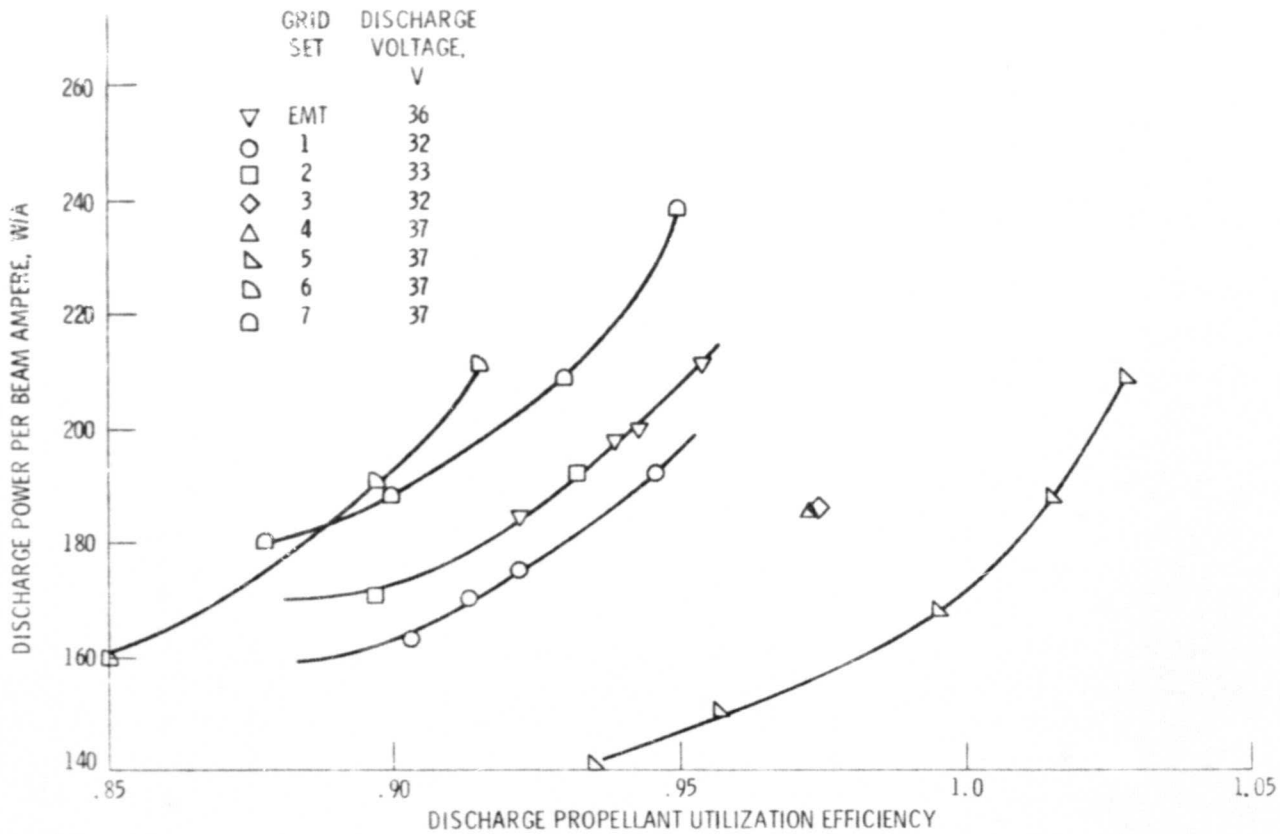

Figure 8. - Discharge losses as a function of discharge propellant utilization efficiency (beam current, 2 A; net voltage, 1100 V; R, 0.69 to 0.76, uncorrected for multiply charged ions).

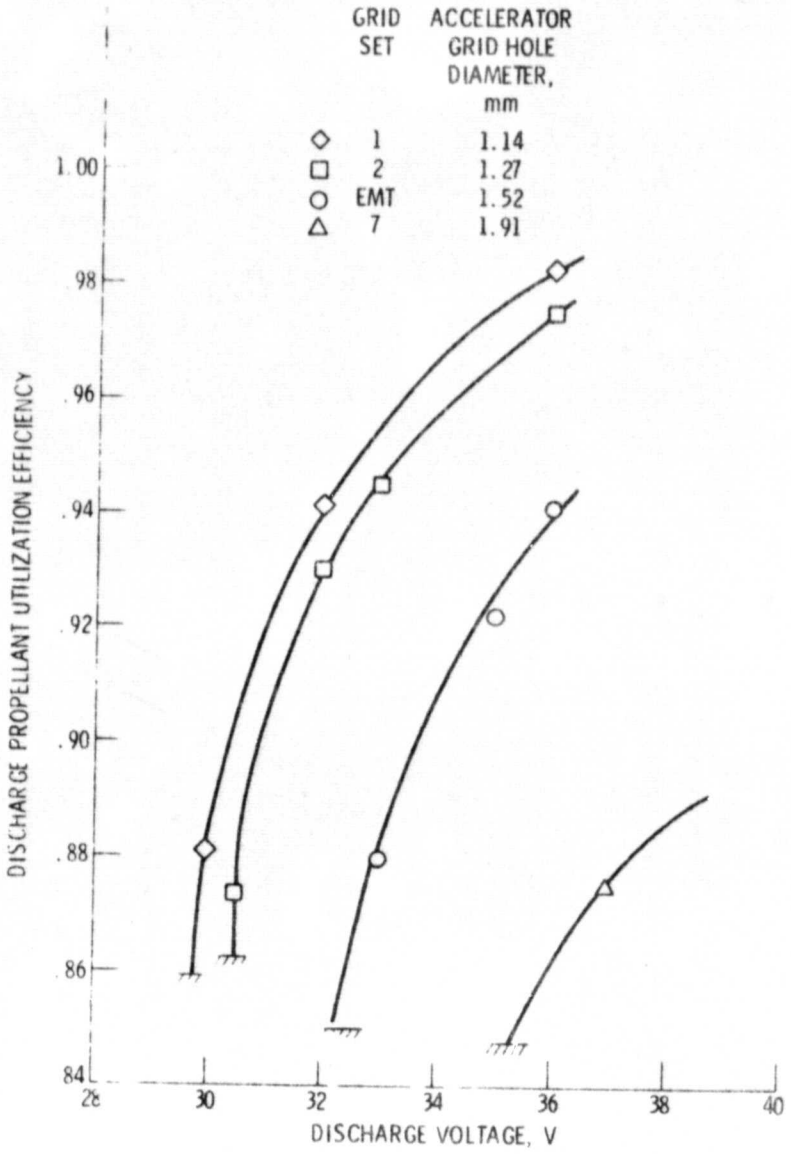

Figure 9. - Discharge propellant utilization efficiency as a function of discharge voltage. (Beam current, 2 A, discharge losses, 200 W/A.)

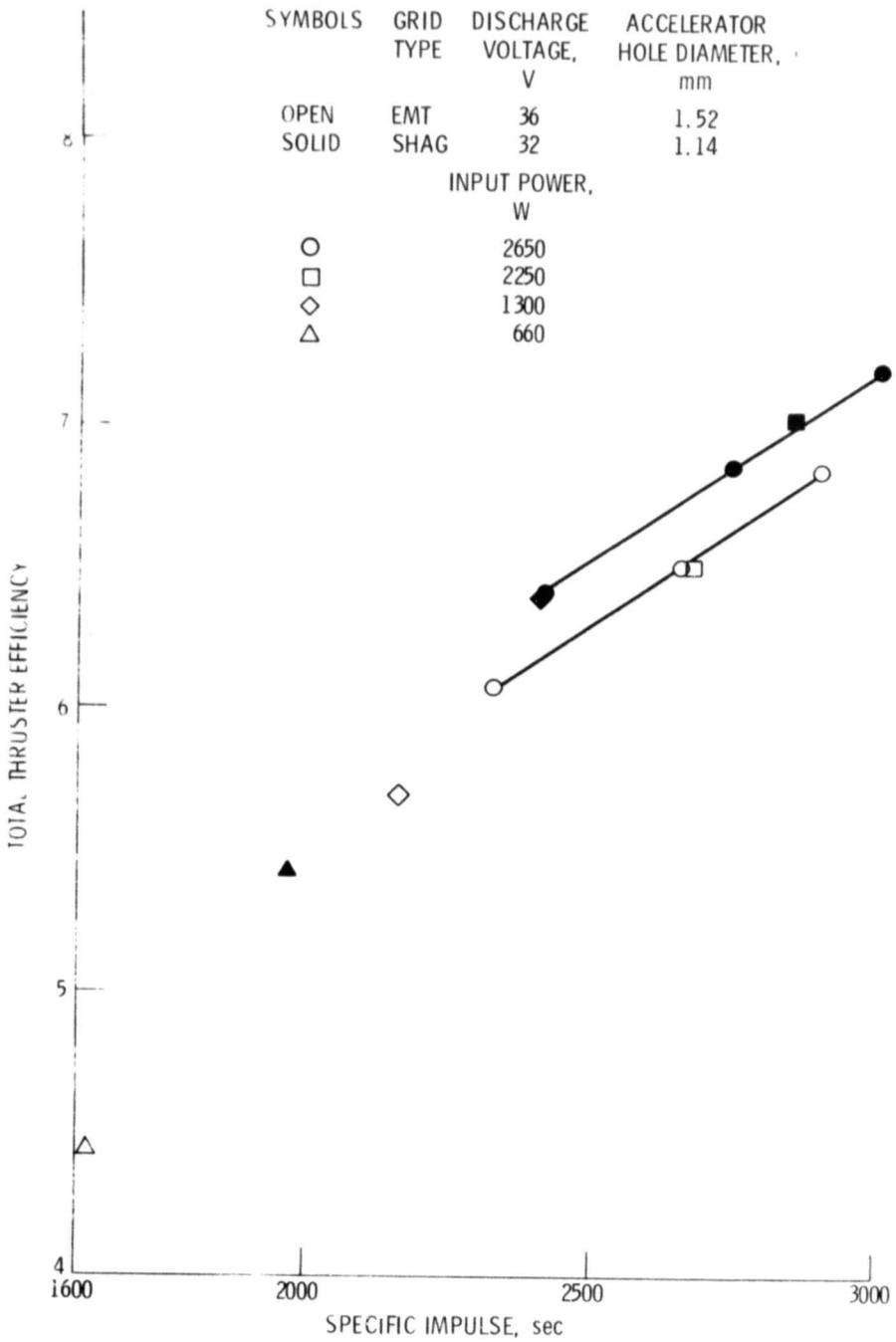

Figure 10. - Total thruster efficiency as a function of specific impulse.